

Communication

Reinforced Materials Based on Chitosan, TiO₂ and Ag Composites

Khairul Anuar Mat Amin and Marc in het Panhuis *

Soft Materials Group, School of Chemistry, University of Wollongong, Northfields Avenue, Wollongong, NSW 2522, Australia; E-Mail: kerol@umt.edu

* Author to whom correspondence should be addressed; E-Mail: panhuis@uow.edu.au; Tel.: +61-242-213-155; Fax: +61-242-214-287.

Received: 30 December 2011; in revised form: 30 January 2012 / Accepted: 8 February 2012 / Published: 16 February 2012

Abstract: This study investigates the mechanical reinforcement of chitosan with TiO₂ and Ag nanoparticles, as well as their water vapour transmission rates and water resistance behaviour. The mechanical properties of chitosan were improved by addition of TiO₂ or Ag, with significant increases in Young's modulus (from 25 MPa to ~300 MPa), tensile strength (from 6 MPa to 18–35 MPa) and toughness (from 1.3 J g^{−1} to 7–8 J g^{−1}). The water vapour transmission rates (368–413 g m^{−2} d^{−1}) were found to be similar for both materials. Inclusion of Ag reduced the water resistance (from 823% to 1,000%), while inclusion of TiO₂ yielded significant improvement in water resistance (from 823% to 100%).

Keywords: chitosan; Ag; TiO₂; nanoparticles; mechanical reinforcement; composite

1. Introduction

Chitosan is a linear cationic polysaccharide derived from chitin, one of the most abundant polysaccharides occurring in nature [1]. Its physical properties have resulted in widespread use in the food, pharmaceutical, and environmental industries [2,3]. For example, chitosan is approved by the United States Environmental Protection Agency as a plant growth extractor to boost plants' ability to defend against fungal infections. Furthermore, it is structurally similar to the extracellular matrix component glycosaminoglycans as well as being biocompatible, biodegradable and antimicrobial [1–4]. The exact mechanism behind chitosan's antimicrobial effect is still under discussion, with several studies pointing towards its ability to enter the bacterial cell wall through pervasion and formation of a polymer membrane on the surface of the cell wall [2,5,6]. The former prevents nutrients from entering

the bacterial cell, while the latter disturbs the physiological activity of the bacterium [6]. Chitosan has been found to be effective against both Gram-negative and Gram-positive bacteria, although its effectiveness depends on its molecular weight, degree of deacetylation (DD) and concentration as well as the surface characteristics of the bacterial cell wall (hydrophilicity and charge) [2,5–8]. For example, chitosan antibacterial effect increases against Gram-positive bacteria with increasing molecular weight, while the reverse was observed for its effectiveness against Gram-negative bacteria [5]. While it has also been determined that positively charged chitosan is more effective against bacteria whose cell wall is predominantly negatively charged [6]. As such, chitosan shows great promise for use as a scaffold in tissue engineering, wound dressing applications, the antimicrobial treatment of textiles as well as water disinfection and microbial control [2,9].

Applications such as food packaging and wound dressings frequently require processing of chitosan into films. This is not straightforward as chitosan is insoluble in most common solvents (including water), but can be overcome by dissolving chitosan in dilute aqueous acidic solutions [10]. It has been established that aqueous acetic acid is one of the most suitable solvents in terms of the resulting film properties such as tensile strength, strain-at-break (extensibility), resistance to water and water vapour permeability [10]. However, the relatively lack of mechanical stiffness and resistance to water of these films (prepared by evaporative casting) has resulted many researchers to seek improvement through physical and chemical methods (such as UV-curing) as well as combining chitosan with clays and nanoparticles [10–13].

Nanoparticles such as titanium dioxide (TiO_2) and silver (Ag) have attracted attention due to their ability to improve mechanical properties, and antibacterial effectiveness against Gram-positive or Gram-negative bacteria and cell growth [9,11,12]. Recent work has shown that combining chitosan or modified chitosan with Ag into composites resulted in films and hydrogels materials with enhanced antimicrobial activity, increased tensile strength but decreased water vapor permeability [14–16]. In other recent work, it was shown that combining chitosan with TiO_2 or Ag nanoparticles yields materials with antibacterial activity against Gram-positive bacterium *Staphylococcus aureus* and *Escherichia coli* as well as displaying promising wound healing characteristics. Most existing reports have prepared chitosan composite films with low Ag/ TiO_2 nanoparticle content, *i.e.*, below 2.5% (by weight relative to chitosan), and focus mostly on cell and antibacterial studies [14,15,17–19]. The mechanical properties (Young's modulus, tensile strength and toughness) of these chitosan-nanoparticle films have not been addressed in detail.

Glycerine (or glycerol, glycerin) is a polyol compound which is widely used in a diverse range of industries. For example, in the food industries it is added as a humectant, while it is also used to produce an essential ingredient (nitro-glycerine) for explosives. Of particular relevance to the research presented in this paper is its usage as a plasticizer to increase polymer film flexibility [20].

In this paper, we investigate the mechanical properties of chitosan, TiO_2 , and Ag composites with nanoparticle content between 10% and 30% (by weight relative to chitosan). We show that water vapour transmission rates and water resistance of our materials is comparable commercial materials.

2. Experimental Section

Chitosan (batch CHM1: medium molecular weight, 75% degree of deacetylation (DD), viscosity \approx 453 cP, product number 448877 - lot number 07918TE; batch CHM2: medium molecular weight, 79% DD, viscosity \approx 915 cP, product number 448877 - lot number 04609LD; and batch CHH: high molecular weight, 75.6% degree of deacetylation, viscosity \approx 1,406 cP, product number 419419 - lot number 10305DD), glycerine, titanium dioxide nanoparticles (diameter, $d < 100$ nm, 99.9% TiO₂, lot number 12908CH) and silver nanoparticles (99.5% Ag, $d < 100$ nm, lot number 07916BH) were obtained from Sigma Aldrich and used as received. Viscosity (1% chitosan in 1% acetic acid) and DD as specified in Sigma-Aldrich's Certificate of Analysis.

2.1. Film Preparation

Chitosan (CH) solutions were prepared by dissolving 2 g chitosan in 90 mL Milli-Q water (resistivity 18.2 M Ω cm) under continuous stirring for 2 h at 70 °C, followed by addition of 10 mL acetic acid (5% v/v). CH-glycerine solutions were prepared by addition of 15%, 30% and 50% of glycerin (by weight relative to CH). CH-TiO₂ and CH-Ag dispersions were prepared by bath sonication (Unisonics FXP 12D, bath volume = 3.3 L, frequency = 40 kHz, power density = 36 mW cm⁻³) of 200 mg, 400 mg, and 600 mg TiO₂ or Ag in 90 mL Milli-Q water for 30 min. This was followed by addition of CH (2 g), glycerine (30% by weight relative to CH) and 10 mL acetic acid (5% v/v) under continuous stirring for 2 h at 70 °C. The resulting TiO₂ and Ag content (by weight relative to CH) are 10%, 20% and 30%.

All films were prepared by evaporative casting. Briefly, a solution was deposited onto an acrylic plate, allowed to dry under controlled ambient conditions (21 °C, 50 \pm 5% relative humidity, RH) for at least 2 days, before peeling off and pre-conditioning in a desiccators under controlled ambient conditions for at least 2 day prior to usage.

2.2. Characterisations of Films

Stress-strain measurements were obtained using an Instron Universal Testing Machine model 8501 with ± 10 kN grips and cross-head speed 20 mm/min. All films were cut into 2.5 cm \times 10 cm samples, while film thickness was measured using a hand-held micrometer (Mitutoyo). Young's modulus, tensile strength, and toughness were calculated from the slope of the linear part of the stress-strain curve, the maximum stress, and by integrating the area under the stress-strain curve, respectively. A minimum of five independent stress-strain measurements were obtained per sample.

The morphology of the composites films was carried out using a field emission scanning electron microscope (JEOL JSM-7500 FA). SEM images of cross-sections were obtained as follows. Samples were freeze-dried in liquid nitrogen (-160 °C), fractured at -150 °C and subsequently were imaged by SEM.

Water resistance was measured by immersing dry films into 150 mL Milli-Q water at 21 °C. After 24 h, the films were removed, wiped gently with a tissue to expel surface water and weighed. Water swelling (WS) was determined from the equilibrium-swelling ratio defined as:

$$WS = (L_{\text{wet}} - L_{\text{dry}})/L_{\text{dry}} \quad (1)$$

where L_{dry} and L_{wet} are the weight of the dry and wet films, respectively. A minimum of five independent measurements were obtained per sample.

The water vapour transmission rate (WVTR) was measured following a modified ASTM International standard method as described previously [21]. Each sample is fixed on the circular opening of a permeation bottle ($d = 1.5$ cm, height = 5.0 cm) with effective transfer area ($A = 1.33$ cm²), and placed in a desiccators (17 °C, 50 ± 5% RH). The WVTR is then determined by measuring the rate of change of mass (m) in these water-filled permeation bottles at exposure times ($\Delta t = 0, 1, 2, 3$ and 4 days) using:

$$WVTR = (m/A \Delta t) \quad (2)$$

where $m/\Delta t$ is the amount of water lost per unit time transfer and A is the area exposed to water transfer (m²).

2.3. Statistical Treatments

The reported results are averages of the four values obtained. Reported numerical errors and graphical error bars are given as ±1 standard deviation (SD). Data and outliers were rejected either when instrumental error was known to have occurred, or if data failed a Q-test with a confidence interval ≥95%.

3. Results and Discussion

Free-standing films (thickness 70–100 µm) were successfully prepared by evaporative casting technique. The resulting films (Figure 1) were robust, flexible and could be easily cut into strips for characterization. The transmittance of CH films is 70% in the visible wavelength range (data not shown). Increasing the film thickness from 70 µm to 100 µm resulted in a reduction in transmittance from 70% to 60% (data not shown). Glycerin (a well-known plasticizer) has been included to improve the brittleness and handle-ability of the films. Increasing the glycerine concentration from 10% to 50% did not reduce the transmittance. Chitosan films incorporated with 0%, 15%, 30% and 50% of glycerine (by weight relative to chitosan) are hereafter referred to as CH0, CH15, CH30 and CH50, respectively. The CH-TiO₂ and CH-Ag films, each of which contained 30% glycerine (by weight relative to CH) were not optically transparent as evident from the photographs in Figure 1(b,c).

Figure 1. Optical images of typical films prepared by evaporative casting of (a) chitosan solution; (b) chitosan-TiO₂ dispersion; and (c) chitosan-Ag dispersion. Dimensions of films are 2.0 cm × 2.0 cm ((a) and (b)) and 3.0 cm × 2.0 cm (c). All films were prepared using chitosan batch CHM1.



The mechanical properties of chitosan (CH0) films, *i.e.*, Young's modulus (E) = $1,223 \pm 173$ MPa, tensile strength (TS) = 39 ± 5 MPa, toughness (T) = 2.45 ± 0.08 J g⁻¹ and strain-at-break (γ) = $10 \pm 2\%$ (Figure 2 and Table 1) are a result of the polymer conformation and the attraction energies (electrostatic attraction, van der Waals forces and hydrogen bonding) between the chitosan chains [17]. Inclusion of glycerine (a well-known plasticizer) significantly reduces the mechanical properties, but increases the strain-at-break hereafter referred to as extensibility (Table 1). For example, addition of 30% glycerine (by weight relative to chitosan) results in a decrease in Young's modulus (from 1223 ± 173 MPa to 25 ± 7 MPa), tensile strength (from 39 ± 5 MPa to 6 ± 1 MPa) and toughness (from 2.45 ± 0.08 J g⁻¹ to 1.27 ± 0.01 J g⁻¹), while the extensibility increased from $10 \pm 1\%$ to $32 \pm 2\%$. This behaviour is in excellent agreement with the well-known plasticizing effect of glycerin [20].

Figure 2. Stress-strain curves for typical chitosan (CH) and chitosan composite films. (a) comparison for glycerine content (by weight relative to CH) of 0% (CH0), 15% (CH15), 30% (CH30) and 50% (CH50); and (b) comparison between composite films containing 10% (by weight relative to CH) of TiO₂ (CHTi10) and Ag (CHAg10). The CHTi10 and CHAg10 films were prepared with 30% glycerine (by weight relative to CH). All films were prepared using chitosan batch CHM1.

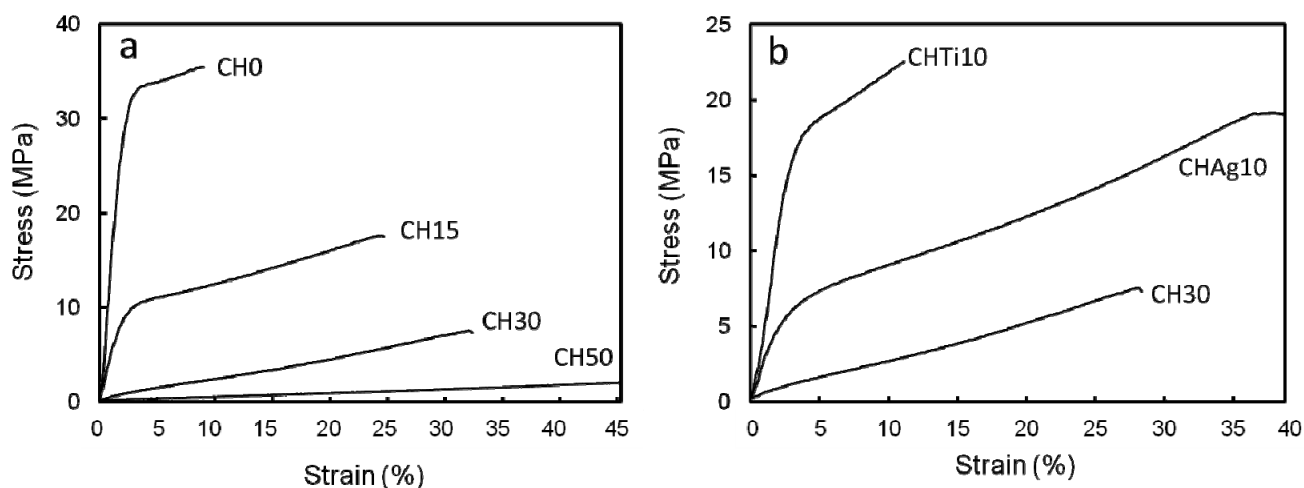


Table 1. Properties of films prepared using chitosan (CH) and glycerine. Glycerine content by weight relative to chitosan (GC), thickness (thick), tensile strength (TS), Young's modulus (E), toughness (T), strain-at-break (γ) and water resistance (WR) for the different CH materials. All films were prepared using chitosan batch CHM1.

Film	GC (%)	Thick (μm)	TS (MPa)	E (MPa)	T (J g^{-1})	γ (%)	WR (%)
CH0	0	70 ± 15	39 ± 5	1223 ± 173	2.45 ± 0.08	10 ± 2	$>>1,000$
CH15	15	72 ± 6	19 ± 8	559 ± 156	4.46 ± 0.32	27 ± 3	$>>1,000$
CH30	30	100 ± 15	6 ± 1	25 ± 7	1.27 ± 0.01	32 ± 2	823 ± 31
CH50	50	116 ± 7	2 ± 1	6 ± 1	0.75 ± 0.05	45 ± 5	331 ± 28

Chitosan is comprised of chains of D-glucosamine with the amount of amino functional groups determined by the degree of deacetylation (DD), *i.e.*, DD = 75% indicates 3 amino functional groups per repeating unit consisting of four saccharide groups. It is well known that the mechanical and physiochemical properties and antimicrobial activity of chitosan depend on a range of factors such as average molecular weight and DD [2,4–6]. The effect of chitosan molecular weight on mechanical values was investigated further by preparing chitosan films with 30% glycerine using: (i) a high molecular weight chitosan (CHH) and (ii) a different batch (CHM2) of the medium molecular weight chitosan product (Table 2). Their DD values are similar, but there is a large difference in viscosity (η) between the different batches of the same medium molecular weight chitosan product, *i.e.*, $\eta = 453$ cP for CHM1 and $\eta = 915$ cP for CHM2. The viscosity of a polymer solution can be related to the molecular weight according to the Mark-Houwink-Sakurada (MHS) equation, which for chitosan has been determined as $\eta = 1.49 \cdot 10^{-4} M_w^{0.79}$ [22]. Hence, the MHS equation suggests that the molecular weights of chitosan CHM2 and CHH batches are 1.7 and 2.4 times that of the CHM1 batch, respectively. These higher molecular weight materials exhibited higher tensile strength and Young's modulus values, see Table 2. The table also shows that our TS and γ values are lower than those reported in the literature for chitosan materials with a higher DD value.

Table 2. Properties of films prepared using chitosan from various sources (Source). Chitosan degree of deacetylation (DD), glycerine content by weight relative to chitosan (GC), tensile strength (TS), Young's modulus (E), strain-at-break (γ) and water resistance (WR) for the different chitosan materials. “CHH” indicates high molecular weight chitosan, while “CHM1” and “CHM2” indicate two different batches of medium molecular weight chitosan, respectively.

Source	DD (%)	H (cP)	GC (%)	TS (MPa)	E (MPa)	γ (%)	WR (%)
CHM1, this work	75	453	30	6 ± 1.0	25 ± 7	32 ± 2	823 ± 31
CHM2, this work	79	915	30	8.0 ± 0.4	100 ± 30	34 ± 2	$>>1,000$
CHH, this work	76	1,406	30	22 ± 4.0	500 ± 134	44 ± 4	268 ± 24
Ref. [10]	>85	-	25	41.6 ± 5.9	-	42.4 ± 4	-
Ref. [14]	90	110	25	32.9 ± 0.7	-	54.6 ± 3	-
Ref. [23]	90	-	28	17.3 ± 2.8	230 ± 5.6	44.2 ± 8	-
Ref. [24]	98	-	20	31.8 ± 2.0	-	45.7 ± 3	-

Glycerin had a significant effect on mechanical properties and also on water resistance (Table 1). Briefly, CH0 and CH15 films showed extensive water swelling ($>>1,000\%$), while CH30 and CH50 resulted in water swelling of $823 \pm 31\%$ and $331 \pm 28\%$, respectively. The extensive swelling behaviour observed for CH0 films can be attributed to electrostatic repulsion between polymer chains. Previously, it has been hypothesised that swelling of CH films can be reduced by, either prevention of chitosan chain movement, or separation of the chains thereby impeding the electrostatic repulsion [25]. It is likely that glycerin's ability to participate in hydrogen bonding may limit chain movement, but further research would be necessary to confirm this suggestion. CH30 offers the best compromise between mechanical properties and water resistance and was adopted for our further investigations into the properties of composites from chitosan, TiO_2 and Ag.

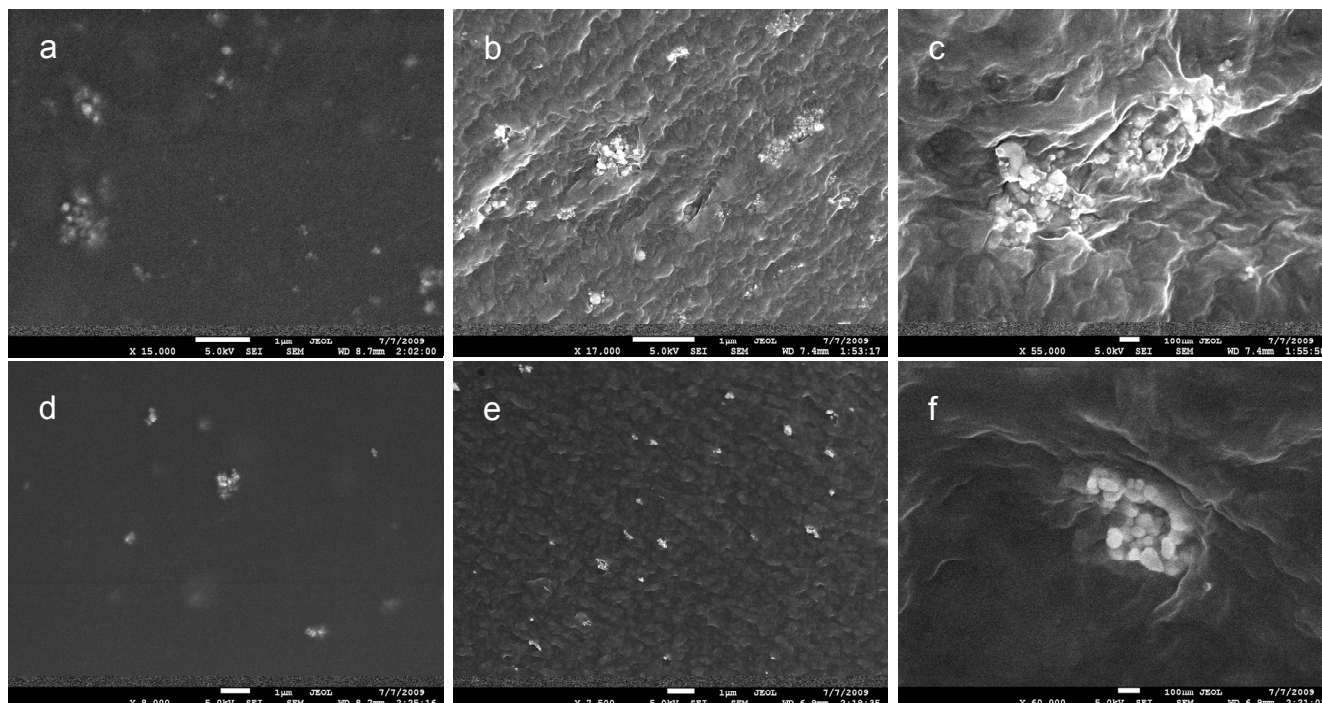
Inclusion of TiO_2 and Ag results in mechanical reinforcement of CH30 materials (Table 3). The mechanical properties of these films increase with increasing TiO_2 and Ag concentration. For example, addition of 30% TiO_2 (by weight relative to CH) results in an 11.8 fold increase in Young's modulus (from 25 ± 7 MPa to 294 ± 11 MPa). The increase in tensile strength and toughness values are both approximately 6 fold, *i.e.*, from 6 ± 1 MPa to 35 ± 6 MPa and from 1.27 ± 0.01 J g⁻¹ to 7.2 ± 1.5 J g⁻¹, respectively, while the extensibility is not affected. Addition of 30% Ag resulted in a 12.9 fold increase in Young's modulus, a 3.0 fold increase in tensile strength and a 6.3 fold increase in toughness, while the extensibility increased marginally (from $32 \pm 2\%$ to $38 \pm 4\%$). Our results demonstrate that CH- TiO_2 materials have significantly higher tensile strength compared to CH-Ag materials (Table 3).

Table 3. Properties of composite films prepared using chitosan, TiO_2 and Ag (Film). Nano-particle content by weight relative to chitosan (NP), tensile strength (TS), Young's modulus (E), toughness (T), strain-at-break (γ), water resistance (WR), thickness (thick) and water vapor transmission rate (WVTR) for the different composite materials. All samples were prepared with 30% glycerin content by weight relative to chitosan. The WVTR for the blank control (no film) returned 439 ± 37 g m⁻² d⁻¹. All films were prepared using chitosan batch CHM1.

Film	NP (%)	Thick (μm)	TS (MPa)	E (MPa)	T (J g ⁻¹)	γ (%)	WR (%)	WVTR (g m ⁻² d ⁻¹)
CH- TiO_2	10	76 ± 3	13 ± 4	99 ± 38	2.45 ± 0.10	24 ± 2	73 ± 11	413 ± 10
	20	79 ± 6	18 ± 1	276 ± 83	4.15 ± 0.42	18 ± 2	100 ± 17	410 ± 11
	30	73 ± 8	35 ± 6	294 ± 11	7.2 ± 1.5	26 ± 4	105 ± 15	408 ± 13
CH-Ag	10	75 ± 8	12 ± 2	103 ± 29	3.24 ± 0.10	33 ± 2	$>>1,000$	383 ± 25
	20	88 ± 20	14 ± 4	310 ± 187	4.1 ± 0.4	35 ± 7	$1,047 \pm 90$	384 ± 26
	30	71 ± 11	18 ± 4	322 ± 145	8.0 ± 1.5	38 ± 4	$1,002 \pm 51$	368 ± 26

Scanning electron microscopy (SEM) was used to investigate the distribution of TiO_2 and Ag nanoparticles in the chitosan matrix. SEM images of the surface and cross-sectional area of the films (Figure 3) show that the nanoparticles are present in small aggregates near the surface, as well as being dispersed throughout the chitosan matrix.

Figure 3. Scanning electron microscopy images of surface (a and d) and cross-sectional areas (b,c and e,f) of typical CH-Ag and CH-TiO₂ composite materials, respectively. Images c and f show an enlarged view of typical nanoparticle aggregates in the composite materials. All films were prepared using chitosan batch CHM1.



In comparison to CH30, the addition of only a small amount of TiO₂ (10%) resulted in a significant reduction in swelling (from $823 \pm 31\%$ to $73 \pm 11\%$), while increasing the TiO₂ to 30% reduced the swelling to $\sim 100\%$, see Tables 1 and 3. In contrast, addition of Ag resulted in the opposite behaviour, *i.e.*, increase in water swelling, which is in agreement with a previous report [14]. Thus, it is clear that addition of TiO₂ further reduces the movement of CH chain, while Ag increases chain movement. The order of magnitude reduction in swelling observed for TiO₂ is likely to arise from its ability to participate in hydrogen bonding with glycerin and chitosan. Whereas, it is suggested that incorporation of Ag may disrupt the effect of glycerin on the CH chains.

Water vapour transmission rates were calculated (using Equation (2)) from water mass loss–time curves (data not shown) and summarized in Table 3. Interestingly, increasing the concentration of the nanoparticles did not significantly decrease the water vapour transmission rates (WVTR), compared to that of the control ($439 \pm 37 \text{ g m}^{-2} \text{ d}^{-1}$). The WVTR for TiO₂ and Ag containing films is in the range of $408\text{--}413 \text{ g m}^{-2} \text{ d}^{-1}$ and $368\text{--}384 \text{ g m}^{-2} \text{ d}^{-1}$, respectively. These values are within the range of WVTR values ($90\text{--}2,893 \text{ g m}^{-2} \text{ d}^{-1}$) reported for eight commercially available synthetic wound dressings [21]. In particular, our values are directly comparable to those reported for the hydrocolloid based dressings IntraSite[®] ($354 \pm 42 \text{ g m}^{-2} \text{ d}^{-1}$) and Restore Cx[®] ($482 \pm 69 \text{ g m}^{-2} \text{ d}^{-1}$).

4. Conclusions

Here we have investigated the mechanical reinforcement of chitosan with TiO₂ and Ag nanoparticles, and their water vapour transmission rates and water resistance behaviour. TiO₂ and Ag

containing composite materials exhibited a significant mechanical reinforcement compared to chitosan films. For example, addition of 30% TiO₂ (by weight relative to chitosan) resulted in an 11.8 fold increase in Young's modulus, a 6 fold increase in tensile strength, and a 6 fold increase in toughness. In comparison, addition of 30% Ag resulted in similar increases in Young's modulus and toughness values, but only a 3 fold increase in tensile strength. The extensibility (strain-at-break) of Ag containing materials was higher compared to that of TiO₂ containing materials.

The water vapour transmission rates were similar for both materials. However, inclusion of Ag lowered the water resistance (increased swelling) of chitosan films, while inclusion of TiO₂ resulted in an order of magnitude improvement in water resistance. On the basis of mechanical characteristics, water vapour transmission rates and water resistance behaviour, films containing TiO₂ nanoparticles result offer more promise for potential future development as components in wound dressing than those with incorporated Ag nanoparticles. This paper contributes to the development of nanoparticle reinforced materials.

Acknowledgments

This work was supported by the University of Wollongong (URC Grant), Australian Research Council (ARC), ARC Future Fellowship (M. in het Panhuis) and Government of Malaysia (K.A. Mat Amin). Tony Romeo thanked for electron microscopy.

References

1. Marguerite, R. Chitin and chitosan: Properties and applications. *Prog. Polym. Sci.* **2006**, *31*, 603–632.
2. Rabea, E.I.; Badawy, M.E.T.; Stevens, C.V.; Smagghe, G.; Steurbaut, W. Chitosan as antimicrobial agent: Applications and mode of action. *Biomacromolecules* **2003**, *4*, 1457–1465.
3. Drury, J.L.; Mooney, D.J. Hydrogels for tissue engineering: scaffold design variables and applications. *Biomaterials* **2003**, *24*, 4337–4351.
4. Tsai, G.J.; Su, W.H.; Chen, H.C.; Pan, C.L. Antimicrobial activity of shrimp chitin and chitosan from different treatments and applications of fish preservation. *Fish. Sci.* **2002**, *68*, 170–177.
5. Chung, Y.-C.; Su, Y.-P.; Chen, C.-C.; Jia, G.; Wang, H.-L.; Wu, J.C.W.; Lin, J.-G. Relationship between antibacterial activity of chitosan and surface characteristics of cell wall. *Acta Pharm. Sin* **2004**, *25*, 932–936.
6. Zheng, L.Y.; Zhu, J.F. Study on antimicrobial activity of chitosan with different molecular weights. *Carbohydr. Polym.* **2003**, *54*, 527–530.
7. Chung, Y.-C.; Chen, C.-Y. Antibacterial characteristics and activity of acid-soluble chitosan. *Bioresour. Technol.* **2008**, *99*, 2806–2814.
8. Wang, X.; Du, Y.; Yang, J.; Wang, X.; Shi, X.; Hu, Y. Preparation, characterization and antimicrobial activity of chitosan/layered silicate nanocomposites. *Polymer* **2006**, *47*, 6738–6744.
9. Li, Q.; Mahendra, S.; Lyon, D.Y.; Brunet, L.; Liga, M.V.; Li, D.; Alvarez, P.J.J. Antimicrobial nanomaterials for water disinfection and microbial control: Potential applications and implications. *Water Res.* **2008**, *42*, 4591–4602.
10. Rhim, J.W.; Weller, C.L.; Ham, K.S. Characteristics of chitosan films as affected by the type of solvent acid. *Food Sci. Biotechnol.* **1998**, *7*, 263–268.

11. Tang, C.; Xiang, L.; Su, J.; Wang, K.; Yang, C.; Zhang, Q.; Fu, Q. Largely improved tensile properties of chitosan film via unique synergistic reinforcing effect of carbon nanotube and clay. *J. Phys. Chem. B* **2008**, *112*, 3876–3881.
12. Tang, C.; Chen, N.; Zhang, Q.; Wang, K.; Fu, Q.; Zhang, X. Preparation and properties of chitosan nanocomposites with nanofillers of different dimensions. *Polym. Degrad. Stab.* **2009**, *94*, 124–131.
13. Podsiadlo, P.; Tang, Z.; Shim, B.S.; Kotov, N.A. Counterintuitive effect of molecular strength and role of molecular rigidity on mechanical properties of layer-by-layer assembled nanocomposites. *Nano Lett.* **2007**, *7*, 1224–1231.
14. Rhim, J.W.; Hong, S.I.; Park, H.M.; Ng, P.K.W. Preparation and characterization of chitosan-based nanocomposite films with antimicrobial activity. *J. Agric. Food Chem.* **2006**, *54*, 5814–5822.
15. Liu, B.S.; Huang, T.B. Nanocomposites of genipin-crosslinked chitosan/silver nanoparticles - structural reinforcement and antimicrobial properties. *Macromol. Biosci.* **2008**, *8*, 932–941.
16. Travan, A.; Pelillo, C.; Donati, I.; Marsich, E.; Benincasa, M.; Scarpa, T.; Semeraro, S.; Turco, G.; Gennaro, R.; Paoletti, S. Non-cytotoxic silver nanoparticle-polysaccharide nanocomposites with antimicrobial activity. *Biomacromolecules* **2009**, *10*, 1429–1435.
17. Sanpui, P.; Murugadoss, A.; Prasad, P.V.D.; Ghosh, S.S.; Chattopadhyay, A. The antibacterial properties of a novel chitosan-Ag-nanoparticle composite. *Int. J. Food Microbiol.* **2008**, *124*, 142–146.
18. Peng, C.C.; Yang, M.H.; Chiu, W.T.; Chiu, C.H.; Yang, C.S.; Chen, Y.W.; Chen, K.C.; Peng, R.Y. Composite nano-titanium oxide–chitosan artificial skin exhibits strong wound-healing effect—an approach with anti-inflammatory and bactericidal kinetics. *Macromol. Biosci.* **2008**, *8*, 316–327.
19. Yuan, W.Y.; Ji, J.; Fu, J.H.; Shen, J.C. A facile method to construct hybrid multilayered films as a strong and multifunctional antibacterial coating. *J. Biomed. Mater. Res. Part B Appl. Biomater.* **2008**, *85B*, 556–563.
20. McHugh, T.H.; Krochta, J.M. Sorbitol- vs. Glycerol-plasticized whey protein edible films: integrated oxygen permeability and tensile property evaluation. *J. Agric. Food Chem.* **1994**, *42*, 842–845.
21. Wu, P.; Fisher, A.C.; Foo, P.P.; Queen, D.; Gaylor, J.D.S. *In vitro* assessment of water vapour transmission of synthetic wound dressings. *Biomaterials* **1995**, *16*, 171–175.
22. Kasaai, M.R.; Arul, J.; Charlet, G. Intrinsic viscosity–molecular weight relationship for chitosan. *J. Polym. Sci. Part B: Polym. Phys.* **2000**, *38*, 2591–2598.
23. Pereda, M.; Aranguren, M.I.; Marcovich, N.E. Characterization of chitosan/caseinate films. *J. Appl. Polym. Sci.* **2008**, *107*, 1080–1090.
24. Suyatma, N.E.; Tighzert, L.; Copinet, A. Effects of hydrophilic plasticizers on mechanical, thermal, and surface properties of chitosan films. *J. Agric. Food Chem.* **2005**, *53*, 3950–3957.
25. Tanabe, T.; Okitsu, N.; Tachibana, A.; Yamauchi, K. Preparation and characterisation of keratin-chitosan composite film. *Biomaterials* **2002**, *23*, 817–825.